



1 **A dual-biomarker approach for quantification of**  
2 **changes in relative humidity from sedimentary lipid D/H**  
3 **ratios**

4  
5 Oliver Rach<sup>1,2</sup>, Ansgar Kahmen<sup>3</sup>, Achim Brauer<sup>4</sup>, Dirk Sachse<sup>1</sup>

6  
7 <sup>1</sup>GFZ – German Research Centre for Geosciences, Section 5.1 Geomorphology, Organic Surface  
8 Geochemistry Lab, Telegrafenberg, 14473 Potsdam (Germany)

9 <sup>2</sup>Institute for Earth- and Environmental Science, University of Potsdam, Karl-Liebknecht-Strasse 24-  
10 25, 14476 Potsdam (Germany)

11 <sup>3</sup>Department of Environmental Sciences-Botany, University of Basel, Schönbeinstrasse 6, CH-4056  
12 Basel (Switzerland)

13 <sup>4</sup>GFZ – German Research Centre for Geosciences, Section 5.2 Climate Dynamics and Landscape  
14 Evolution, Telegrafenberg, 14473 Potsdam (Germany)

15  
16 *Correspondence to:* Oliver Rach ([oliver.rach@gfz-potsdam.de](mailto:oliver.rach@gfz-potsdam.de))

17  
18 **Abstract**

19 Past climatic change can be reconstructed from sedimentary archives by a number of proxies.  
20 However, few methods exist to directly estimate hydrological changes and even fewer result in  
21 quantitative data, impeding our understanding of the timing, magnitude and mechanisms of  
22 hydrological changes.

23 Here we present a novel approach based on  $\delta^2\text{H}$  values of sedimentary lipid biomarkers in combination  
24 with plant physiological modeling, to extract quantitative information on past changes in relative  
25 humidity. Our initial application to an annually laminated lacustrine sediment sequence from western  
26 Europe deposited during the Younger Dryas cold period revealed relative humidity changes of up to  
27 15% over sub-centennial timescales, leading to major ecosystem changes, in agreement with  
28 palynological data from the region. We show that by combining organic geochemical methods and  
29 mechanistic plant physiological models it is possible to extract quantitative ecohydrological parameters  
30 from sedimentary lipid biomarker  $\delta^2\text{H}$  data.

31  
32 **1. Introduction**

33  
34 Predicting future changes in the water cycle using state-of-the art climate models is still associated with  
35 large uncertainties (IPCC, 2015). This is because we lack a mechanistic understanding of some of the  
36 key processes that influence the water cycle, in particular at regional spatial scales. A better  
37 mechanistic understanding of drivers and feedbacks within the hydrological cycle can be achieved from



38 reconstructing past hydrological changes from sedimentary archives. Stable isotope ratios of meteoric  
39 water, expressed as  $\delta^{18}\text{O}$  and  $\delta^2\text{H}$  ( $\delta\text{D}$ ) values are an excellent tool in this respect, because their  
40 variability is associated with changes in temperature and source water (Bowen, 2008; Gat, 1996). The  
41 isotope ratios of precipitation can be recorded in ice core (Alley, 2000), terrestrial and marine  
42 paleoclimate archives through a variety of proxies, such as carbonates (Kanner et al., 2013; von  
43 Grafenstein et al., 1999), silicates (Tyler et al., 2008) and lipid biomarkers (Sachse et al., 2012).

44 Despite their potential, the interpretation of the stable isotope ratios from inorganic and organic proxies  
45 often allows only a *qualitative* assessment of past hydrological changes while *quantitative*  
46 reconstructions of hydrological changes from isotope proxy data, such as precipitation amount or  
47 relative humidity, have been difficult to achieve. This is problematic as quantifiable data are necessary  
48 for identifying the mechanistic drivers of past hydroclimate changes as well as their continental scale  
49 feedbacks and thresholds for example for vegetation changes. Moreover, quantitative data are needed  
50 to test the performance of state-of-the-art climate models in simulating past and future changes in the  
51 hydrological cycle.

52 The interpretation of isotope proxies is typically not quantitative because multiple drivers can influence  
53 meteoric  $\delta^{18}\text{O}$  and  $\delta^2\text{H}$  values, hampering the assignment of single quantitative relationships between a  
54 hydrologic variable and  $\delta^2\text{H}$  values recorded in a geological archive (Alley and Cuffey, 2001). To  
55 overcome this limitation, we present a new approach that combines lipid biomarker hydrogen isotope  
56 measurements and plant physiological modeling to constrain the influence of multiple drivers on  $\delta^2\text{H}$   
57 values recorded in organic material and allow thus to extract quantitative information about changes in  
58 relative humidity from sedimentary archives.

59 Over the past decade,  $\delta^2\text{H}$  values of lipid biomarkers from photosynthetic organisms have been  
60 increasingly used as proxies for reconstructing past changes in the continental hydrological cycle  
61 (Feakins, 2013; Rach et al., 2014; Sachse et al., 2012; Schefuss et al., 2011; Seki et al., 2011). In  
62 particular *n*-alkanes are ubiquitous in marine and lacustrine sediments and can be preserved over  
63 geological timescales (Peters et al., 2007). *n*-Alkanes can be traced back to aquatic or terrestrial  
64 sources, where short-chain homologues ( $n\text{C}_{17}$ - $n\text{C}_{21}$ ) are primarily synthesized by algae and aquatic  
65 plants (Aichner et al., 2010; Ficken et al., 2000), mid-chain *n*-alkanes (e.g.  $n\text{C}_{23}$ - $n\text{C}_{25}$ ) by submerged  
66 aquatic macrophytes or mosses (Aichner et al., 2010; Ficken et al., 2000; Gao et al., 2011), and long-  
67 chain *n*-alkanes ( $>n\text{C}_{25}$ ) predominantly by higher terrestrial plants as a protective leaf wax layer on the  
68 leaf surface (Bush and McInerney, 2013; Eglinton and Hamilton, 1967).

69 Algae and submerged aquatic plants directly use lake (or ocean) water as their hydrogen source for  
70 lipid synthesis.  $\delta^2\text{H}$  values from *n*-alkanes from aquatic organism ( $\delta^2\text{H}_{\text{aq}}$ ) are thus related to the  $\delta^2\text{H}$   
71 value of the water these organisms live in (Aichner et al., 2010; Sachse et al., 2004) offset by a  
72 biosynthetic fractionation ( $\epsilon_{\text{bio}}$ ) between water and *n*-alkanes (Sachse et al., 2012) (Eq. (1)). Laboratory  
73 culture studies (Zhang and Sachs, 2007) as well as field studies (Aichner et al., 2010; Sachse et al.,  
74 2004) have resulted in strong linear and nearly 1:1 relationships between source water and  $\delta^2\text{H}_{\text{aq}}$   
75 (Sachse et al., 2012), but have shown that species specific differences in  $\epsilon_{\text{bio}}$  do exist (Zhang and Sachs,  
76 2007).

77



$$(1) \delta^2\text{H}_{aq} = \delta^2\text{H}_{precip} + \epsilon_{bio}$$

78

79 Terrestrial plant leaf wax *n*-alkane  $\delta^2\text{H}$  values ( $\delta^2\text{H}_{terr}$ ) have also been found to be linearly correlated to  
 80 the organisms source water  $\delta^2\text{H}$  values, yet not in a 1:1 relationship (Sachse et al., 2012), indicating  
 81 additional influences on  $\delta^2\text{H}_{terr}$  values. Recent greenhouse experiments and field studies have revealed  
 82 that in particular the evaporative  $^2\text{H}$  enrichment of leaf water shapes  $\delta^2\text{H}_{terr}$  values (Kahmen et al.,  
 83 2013a; Kahmen et al., 2013b). Soil water evaporation in the upper soil layers has been shown to be less  
 84 significant for  $\delta^2\text{H}_{terr}$ , as plants usually access the deeper, isotopically unenriched, soil layers (Dawson,  
 85 1993). As such,  $\delta^2\text{H}_{terr}$  is affected mainly by the  $\delta^2\text{H}$  value of plant source water (i.e. precipitation), the  
 86 biosynthetic fractionation and leaf water deuterium enrichment ( $\Delta^2\text{H}_e$ ) (Eq. (2)).

87

$$(2) \delta^2\text{H}_{terr} = \delta^2\text{H}_{precip} + \Delta^2\text{H}_e + \epsilon_{bio}$$

88

89 Systematic differences in  $\delta^2\text{H}_{terr}$  values have been observed for different plant types (especially  
 90 between grasses and trees) (Diefendorf et al., 2011; Kahmen et al., 2013b), possibly indicating  
 91 differences in either  $\epsilon_{bio}$  (Sachse et al., 2012) or the fraction of leaf water used for lipid biosynthesis  
 92 (Kahmen et al., 2013b) or yet unidentified factors. As such, vegetation changes in sedimentary records  
 93 have been suggested to affect  $\delta^2\text{H}_{terr}$  values and “vegetation corrections” have been proposed (Feakins,  
 94 2013).

95 Since evaporative  $^2\text{H}$  enrichment of leaf water only affects terrestrial plants but not aquatic organisms,  
 96 changes in sedimentary  $\delta^2\text{H}_{terr}$  (Sachse et al., 2006) can be seen as a record of variations in terrestrial  
 97 evaporative  $^2\text{H}$  enrichment over time. Thus, by combining Eq. (1) and (2) under the assumption that  $\epsilon_{bio}$   
 98 of both aquatic and terrestrial organisms was constant on the temporal and spatial scales of sedimentary  
 99 integration, the difference between  $\delta^2\text{H}_{aq}$  and  $\delta^2\text{H}_{terr}$  values should mainly reflect the evaporative  $^2\text{H}$   
 100 enrichment of leaf water (Eq. (3)).

101

$$(3) \Delta^2\text{H}_e = \delta^2\text{H}_{terr} - \delta^2\text{H}_{aq}$$

102

103 Variants of this concept (Sachse et al., 2004) have been used to qualitatively interpret changes in  
 104 evapotranspiration through the isotopic difference between  $\delta^2\text{H}_{terr}$  and  $\delta^2\text{H}_{aq}$  (i.e. expressed as  $\alpha_{TA/wat}$ ,  
 105  $\delta^2\text{H}_{C_{23}-C_{31}}$  and  $\epsilon_{terr-aq}$  (Jacob et al., 2007; Rach et al., 2014; Seki et al., 2011)). With recent progress in  
 106 understanding of the determinants of  $\delta^2\text{H}_{terr}$  values and the existing mechanistic understanding of the  
 107 processes governing leaf water evaporative  $^2\text{H}$  enrichment (Craig, 1965; Kahmen et al., 2011b; Sachse  
 108 et al., 2012), we propose a new framework – which we term the dual-biomarker (DUB) approach - to  
 109 extract quantitative hydrological information, namely changes in relative humidity ( $\Delta rh$ ) from  
 110 sedimentary records. To illustrate the power of this approach with paleohydrological data, we combine  
 111 compound-specific hydrogen isotope measurements with plant physiological modeling on a previously  
 112 published Late Glacial record of  $\delta^2\text{H}_{aq}$  and  $\delta^2\text{H}_{terr}$  from sediments of Lake Meerfelder Maar (MFM),  
 113 Germany (Rach et al., 2014).

114



## 115 2. Approach and Model

116

117 The DUB approach for quantifying changes in relative humidity from aquatic and terrestrial lipid  
 118 biomarker  $\delta^2\text{H}$  values is based on the assumption, that lake water evaporation is minimal in small  
 119 catchment lakes from temperate regions (Sachse et al., 2006).  $\delta^2\text{H}_{\text{aq}}$  can thus be regarded as a direct  
 120 recorder of growing season average precipitation  $\delta^2\text{H}$  values. We further argue that  $\delta^2\text{H}_{\text{terr}}$  values  
 121 largely reflect leaf water  $\delta^2\text{H}$  values as has recently been demonstrated for greenhouse and field grown  
 122 plants (Kahmen et al., 2013a; Kahmen et al., 2013b). Leaf water in turn is a function of the plant's  
 123 source water and leaf water evaporative  $^2\text{H}$  enrichment. We argue that soil water evaporation is  
 124 negligible as recently suggested by several observational studies and a global assessment (Jackson et  
 125 al., 1996; Jasechko et al., 2013; Kahmen et al., 2013a) and that precipitation is the ultimate water  
 126 source of aquatic organisms and terrestrial plants. In terrestrial plants however, the source water  
 127 becomes more enriched in deuterium due to plant transpiration before it is used for lipid biosynthesis.  
 128 As such, the isotopic difference between  $\delta^2\text{H}_{\text{terr}}$  and  $\delta^2\text{H}_{\text{aq}}$  ( $\varepsilon_{\text{terr-aq}}$ ) can be attributed to mean leaf water  
 129 evaporative  $^2\text{H}$  enrichment ( $\Delta^2\text{H}_e$ ) (Sachse et al., 2004). Based on recent field and greenhouse studies  
 130 we further assume, that  $\varepsilon_{\text{terr-aq}}$  captures a growing season signal, probably biased towards the earlier  
 131 summer months in temperate climate zones as the majority of leaf waxes is produced during leaf  
 132 development with suggested integrational periods between weeks (Kahmen et al., 2013b; Tipple et al.,  
 133 2013) and several months (Sachse et al., 2015).

134

135 The major variables controlling leaf water isotope enrichment are well understood and mechanistic  
 136 models have been developed based on the Craig-Gordon evaporation model (Craig, 1965) that allow to  
 137 accurately predict or reconstruct leaf water  $\Delta^2\text{H}_e$  values based on environmental and physiological  
 138 input variables (Barbour, 2007; Farquhar et al., 2007; Ferrio et al., 2009; Kahmen et al., 2011b) (Eq.  
 139 (4))

$$(4) \quad \Delta^2\text{H}_e = \varepsilon_+ + \varepsilon_k + (\Delta^2\text{H}_{\text{wv}} - \varepsilon_k) \frac{e_a}{e_i}$$

140

141  $\Delta^2\text{H}_e$  is determined by the equilibrium isotope fractionation between liquid and vapor ( $\varepsilon_+$ ), the kinetic  
 142 isotope fractionation during water vapor diffusion from the leaf intercellular air space to the  
 143 atmosphere ( $\varepsilon_k$ ), the  $^2\text{H}$  depletion of water vapor relative to source water ( $\Delta^2\text{H}_{\text{wv}}$ ), and the ratio of  
 144 atmospheric vapor pressure and intracellular vapor pressure ( $e_a/e_i$ ) and air temperature ( $T_{\text{air}}$ ). In  
 145 addition, leaf temperature ( $T_{\text{leaf}}$ ), stomatal conductance ( $g_s$ ) and boundary layer resistance ( $r_b$ ) are  
 146 essential secondary input variables for the prediction of  $e_i$  and  $\varepsilon_k$ , respectively. Reformulating Eq. (4)  
 147 allows expressing  $e_a$  as a function of Craig-Cordon variables (Eq. (5)). Since the atmospheric vapor  
 148 pressure  $e_a$  can also be calculated based on rh and  $e_{\text{sat}}$  (Eq. (6)) we can merge Eq. (5) and (6) to  
 149 calculate relative humidity (rh) and to estimate quantitative changes in rh ( $\Delta\text{rh}$ ) (Eq. (7)).

150

$$(5) \quad e_a = \frac{e_i(\Delta^2\text{H}_e - \varepsilon_+ - \varepsilon_k)}{\Delta^2\text{H}_{\text{wv}} - \varepsilon_k}$$

151



$$(6) \text{ rh} = \frac{e_a \cdot 100\%}{e_{sat}}$$

152

$$(7) \Delta \text{rh} = \frac{e_i(\Delta^2 H_e - \varepsilon_+ - \varepsilon_k) \cdot 100\%}{e_{sat}(\Delta^2 H_{wv} - \varepsilon_k)}$$

153

154 Equation (7) illustrates that  $\Delta \text{rh}$  can be inferred from a record of past changes in  $\Delta^2 H_e$  (i.e. a record of  
 155  $\varepsilon_{\text{terr-aq}}$ ) if the additional variables  $e_{sat}$ ,  $e_i$ ,  $\Delta^2 H_{wv}$ ,  $\varepsilon_+$  and  $\varepsilon_k$  can be constrained. In the following we discuss  
 156 the model parameterizations necessary to apply the DUB approach to estimate quantitative changes in  
 157  $\text{rh}$  from sedimentary records.

158

159 Saturation vapor pressure  $e_{sat}$  (Eq. (8)) as well as the equilibrium fractionation factor  $\varepsilon_+$  (Eq. (9)) are a  
 160 function of temperature. The atmospheric pressure term ( $e_{atm}$ ), which is also needed for calculation of  
 161  $e_{sat}$ , describes the atmospheric pressure depending on the elevation above sea level (0 meters = 1013  
 162 hPa).

$$(8) e_{sat} = \frac{1.0007 + 3.46 \cdot e_{atm}[\text{hPa}]}{1000000} \cdot 6.1121 \cdot \exp\left(\frac{17.502 \cdot T_{air}[\text{°C}]}{240.97 + T_{air}[\text{°C}]}\right)$$

163

$$(9) \varepsilon_+ = \left[ \exp\left(\frac{24.844 \cdot 1000}{(273.16 + T_{air}[\text{°C}])^2} - \frac{76.248}{273.16 + T_{air}[\text{°C}]} + 0.052612\right) - 1 \right] \cdot 1000$$

164

165 For accurate estimates of  $e_{sat}$  as well as  $\varepsilon_+$  information on air temperature ( $T_{air}$ ) during the growing  
 166 season is thus required. Estimates of past  $T_{air}$  variability can be derived from paleotemperature proxy  
 167 data to estimate  $e_{sat}$  and  $\varepsilon_+$  (e.g. chironomids (Heiri et al., 2014; Heiri et al., 2007), MBT/CBT (Blaga et  
 168 al., 2013)). In particular chironomid records, thought to represent spring and summer temperatures,  
 169 provide an ideal proxy of past mean growing season temperatures in this respect (Heiri et al., 2007).  
 170 Note that  $e_{sat}$  also depends on the atmospheric pressure (Eq. (8)), which can be estimated from  
 171 elevation above sea level and is treated as a constant in the model. Leaf-internal vapor pressure  $e_i$   
 172 on the other hand is a function leaf temperature ( $T_{leaf}$ ). We assume for our calculations that  $T_{air}$  is a good  
 173 estimate of a growing season average  $T_{leaf}$  and  $e_i$  can thus be calculated as:

174

$$(10) e_i = 6.13753 \cdot \exp\left(T_{air}[\text{°C}] \cdot \frac{18.564 - \frac{T_{air}[\text{°C}]}{254.4}}{T_{air}[\text{°C}] + 255.57}\right)$$

175

176 We are aware that  $T_{leaf}$  can exceed air temperature in situations of extreme drought, when transpiration  
 177 and evaporative cooling is reduced, or in bright and sunny conditions (Leuzinger and Komer, 2007;  
 178 Scherrer et al., 2011). However, on cloudy days as well as on days with wind,  $T_{leaf}$  typically equals  $T_{air}$   
 179 (Jones, 2013). Given the spatial and temporal integration of leaves in sedimentary records (covering  
 180 decadal to millennial timescales) it is thus unlikely that single drought events, where  $T_{leaf}$  would exceed



181  $T_{\text{air}}$  dominate the overall relationship between  $T_{\text{leaf}}$  and  $T_{\text{air}}$  and we thus assume that using  $T_{\text{air}}$  as a proxy  
 182 for  $T_{\text{leaf}}$  introduces little error into our calculations.

183 Another parameter affecting leaf water isotope enrichment is the  $^2\text{H}$ -depletion of water vapor relative  
 184 to source water ( $\Delta^2\text{H}_{\text{wv}}$ ). In temperate climates liquid water and atmospheric water vapor are often in  
 185 isotopic equilibrium, especially when longer (annual to decadal) timescales are investigated (Jacob and  
 186 Sonntag, 1991). We therefore assume that  $\Delta^2\text{H}_{\text{wv}}$  equals the equilibrium isotope fractionation between  
 187 vapor and liquid  $\epsilon_+$ .

$$(11) \quad \Delta^2\text{H}_{\text{wv}} = -\epsilon_+$$

188

189 In the model,  $\Delta^2\text{H}_{\text{wv}}$  can thus be replaced by  $-\epsilon_+$  (Eq. (11)).

190 The kinetic isotope fractionation ( $\epsilon_k$ ) depends on the plant physiological variables stomatal  
 191 conductance ( $g_s$ ) and boundary layer resistance ( $r_b$ ) (Eq. (12)) (Kahmen et al., 2011b).

192

$$(12) \quad \epsilon_k = \frac{16.4 \cdot \frac{1}{g_s [\text{mol}/\text{m}^2/\text{s}]} + 10.9 \cdot r_b [\text{mol}/\text{m}^2/\text{s}]}{\frac{1}{g_s [\text{mol}/\text{m}^2/\text{s}]} + r_b [\text{mol}/\text{m}^2/\text{s}]}$$

193

194 No direct proxies exist to reconstruct these plant physiological variables from sedimentary records, but  
 195 paleovegetation data can be used to parameterize the model with biome-averaged values for  $g_s$  and  $r_b$   
 196 that are inferred from modern plants (Klein, 2014). We note that these plant physiological variables  
 197 exert only minor control on the model outcome, expected to lie within the analytical error of  $\delta^2\text{H}$  lipid  
 198 measurements (Kahmen et al., 2011b), see also discussion below.

199 The latest iterations of leaf water models also include a Péclet effect, which describes the ratio of  
 200 convectional versus diffusional flow of water in the leaf (Eq. (4))(Kahmen et al., 2011b). We did,  
 201 however, not include the Péclet effect in our calculations because we assume that variations in the  
 202 Péclet effect are minimal over time (Kahmen et al., 2009; Song et al., 2013) in particular for  
 203 angiosperm species.

204 When combining Eq. (9), (10), (11) and (12) with Eq. (7), we obtain a model for  $\Delta\text{rh}$  that requires only  
 205 four input variables:  $\epsilon_{\text{terr-aq}}$ , air temperature ( $T_{\text{air}}$ ) as well as literature-derived values for stomatal ( $g_s$ )  
 206 and boundary layer conductance ( $r_b$ ) to calculate  $\Delta\text{rh}$ :

207

$$(13) \quad \Delta\text{rh} = e_i'(T_{\text{air}}) \cdot \left( \frac{\Delta^2\text{H}_e}{-e_{\text{sat}}'(e_{\text{atm}}, T_{\text{air}})(\epsilon_+(T_{\text{air}}) + \epsilon_k'(g_s, r_b))} + \frac{1}{e_{\text{sat}}'(e_{\text{atm}}, T_{\text{air}})} \right) \cdot 100\%$$

208

209 Since we use  $\epsilon_{\text{aq-terr}}$  ( $=\Delta^2\text{H}_e$ ) as an input variable, which is representative of leaf water isotope  
 210 enrichment above source water and not absolute  $\delta^2\text{H}$  leaf water values, Eq. (13) predicts changes in rh  
 211 ( $\Delta\text{rh}$ ) but not rh directly. In theory, Eq. (13) would also allow the calculation of rh values directly, if  
 212 absolute  $\delta^2\text{H}_{\text{precip}}$  and  $\delta^2\text{H}_{\text{leafwater}}$  was available. The current lack of experimentally determined  
 213 biosynthetic fractionation factors for the respective aquatic and terrestrial plants prevents this approach,  
 214 but future experimental research may result in robust estimates of  $\epsilon_{\text{bio}}$ , enabling the reconstruction of  
 215 absolute rh values (Zhang et al., 2009).



### 216 3. Uncertainties and sensitivity tests

217

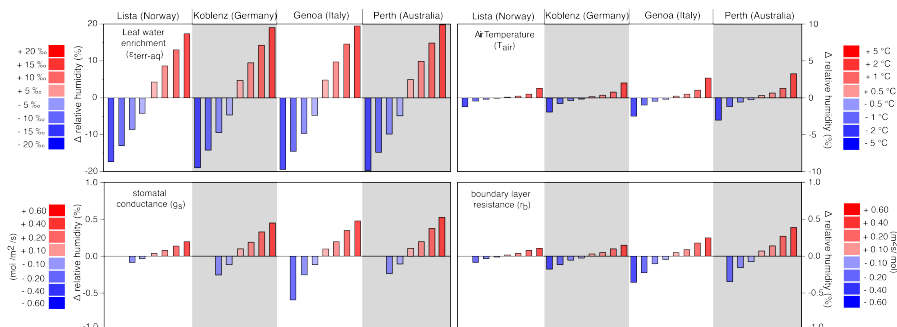
218 Although the DUB approach for estimating  $\Delta rh$  is based on only four input variables, these variables  
 219 still have to be derived from other proxies and our assumptions are associated with uncertainties. To  
 220 evaluate the robustness of our DUB approach for predicting  $\Delta rh$  in the context of these uncertainties,  
 221 we tested the sensitivity of the model to uncertainties in the four key input variables  $T_{air}$ ,  $\epsilon_{terr-aq}$ ,  $g_s$  and  
 222  $r_b$ . In these sensitivity analyses we used a leaf water model, where all secondary variables ( $e_i$ ,  $e_k$ ,  $e_+$ ,  $e_{sat}$ )  
 223 are coupled to the primary input variables  $T_{air}$ ,  $T_{leaf}$ ,  $g_s$  and  $r_b$  (Kahmen et al., 2011b). We performed  
 224 this test under a range of dramatically different climatic and ecological settings reflected by the climate  
 225 conditions of Lista (Norway), Koblenz (Germany), Genoa (Italy) and Perth (Australia) that differ in  
 226 mean growing season temperatures and prevailing vegetation types. While the vegetation in Norway  
 227 and Australia is dominated by conifers and Mediterranean shrubland respectively, the prevailing  
 228 vegetation in Germany and Italy are broad leaf tree species. As baseline values for the sensitivity tests  
 229 we set  $T_{air}$  in the analyses to the growing season mean temperatures of each site, which was 9.4°C,  
 230 15°C, 17.2°C and 20.4°C for Lista, Koblenz, Genoa and Perth respectively (IAEA/WMO, 2006). Leaf  
 231 water evaporative enrichment  $\epsilon_{terr-aq}$  ( $\Delta^2H_e$ ) was set to 25‰ (Lista), 35‰ (Koblenz), 45‰ (Genoa) and  
 232 55‰ (Perth), which reflects average growing season leaf water enrichment values for the tested  
 233 environments (Kahmen et al., 2013a). Base line data for plant physiological variables were biome  
 234 typical estimates that we obtained from the literature (Jones, 2013; Klein, 2014): stomatal conductance  
 235 ( $g_s$ ) for Lista and Koblenz was set to 0.25 mol/m<sup>2</sup>/s, while for Genoa and Perth the preset values were  
 236 0.45 and 0.35 mol/m<sup>2</sup>/s, respectively (Klein, 2014). Boundary layer resistance ( $r_b$ ) for Lista and Perth  
 237 was set to 0.5 m<sup>2</sup>/s/mol, while for Koblenz and Genoa this variable was set to 1.0 m<sup>2</sup>/s/mol (Jones,  
 238 2013).

239 The temperature sensitivity tests were performed by increasing and decreasing the respective  $T_{air}$   
 240 values for a location by 0.5°C, 1°C, 2°C and 5°C. For the  $\epsilon_{terr-aq}$  ( $\Delta^2H_e$ ) the respective  $\epsilon_{terr-aq}$  ( $\Delta^2H_e$ )  
 241 values were varied by  $\pm 5\%$ , 10%, 15% and 20% for each location. The plant physiological variables  
 242 ( $g_s$  and  $r_b$ ) were varied by  $\pm 0.1$ ,  $\pm 0.2$ ,  $\pm 0.4$  and in maximum by  $\pm 0.6$  mol/m<sup>2</sup>/s and  $\pm 0.6$  m<sup>2</sup>/s/mol,  
 243 respectively. These tested variations in plant physiological variables cover the expected variation in  $g_s$   
 244 and  $r_b$  for the local vegetation at a site.

245 The sensitivity analyses showed similar results for all four tested environments (Fig. 1). This suggests a  
 246 similar behavior of the model under very different climate and ecological conditions. The DUB model  
 247 is most sensitive to changes in  $\epsilon_{terr-aq}$  (i.e.  $\Delta^2H_e$ ) and  $T_{air}$ , while the plant physiological variables ( $g_s$ ,  $r_b$ )  
 248 showed only minor effects on  $\Delta rh$  (Fig 1). Specifically, a change of  $\pm 20\%$  in  $\epsilon_{terr-aq}$  (i.e.  $\Delta^2H_e$ ) resulted  
 249 in a change  $\pm 20\%$  in  $\Delta rh$ . A  $\pm 5^\circ\text{C}$  change in  $T_{air}$  resulted in a 3% change in  $\Delta rh$ . Varying  $g_s$  and  $r_b$   
 250 within the specified limits caused only changes in  $\Delta rh$  of 0.01 to 0.5% (Fig. 1), suggesting low model  
 251 sensitivity to plant physiological variables. The difference in calculated  $\Delta rh$  for sites with low (e.g.  
 252 Lista) and high (e.g. Perth) growing season mean temperature were smaller than the regional model  
 253 sensitivity of the different input variables and are therefore negligible. Our sensitivity analyses shows  
 254 that the most critical variables for estimating changes in relative humidity with our model are  $\epsilon_{terr-aq}$  and  
 255  $T_{air}$  (Fig 1).



256



257

258 **Fig 1.** Sensitivity analyses for major model input variables ( $\epsilon_{\text{terr-aq}}$ ,  $T_{\text{air}}$ ,  $g_s$  and  $r_b$ ) on resulting  $\Delta rh$   
 259 values tested for four different climatic and ecological environments (Norway, Germany, Italy and  
 260 Australia). Bars represent the effect on model output ( $\Delta rh$ ) for each tested environment and its variation  
 261 when the respective input variable will be varied by the marked value. Missing bars (i.e. for negative  $g_s$   
 262 and  $r_b$ ) results from a bigger (negative) variation than the preset value (below 0).

263

264 **4. Application: Reconstructing quantitative changes in  $\Delta rh$  during the Younger Dryas (YD) in**  
 265 **Western Europe**

266

267 To illustrate the potential of the DUB approach for estimating changes in  $rh$  over time, we applied the  
 268 model using a previously published high-resolution dataset of  $\delta^2H_{\text{terr}}$  and  $\delta^2H_{\text{aq}}$  values from lake  
 269 Meerfelder Maar (MFM) in W-Germany (Rach et al., 2014). This record was interpreted to depict  
 270 significant hydroclimate variability during the onset and the termination of the Younger Dryas (YD)  
 271 period in Western Europe between ca. 13.100 and 11.000 years BP. The availability of additional  
 272 different proxy data, such as palynological data (Brauer et al., 1999a; Litt and Stebich, 1999), enables a  
 273 robust parameterization of the DUB model for the MFM sediment record. In addition, annual varves  
 274 and a high temporal sampling resolution (decades) allow the evaluation of the timing of climatic and  
 275 ecosystem changes - an ideal setting to illustrate the power of the DUB approach. A detailed  
 276 description of the record and the available proxy data are given in Rach et al. (2014). Briefly, the  
 277 annually laminated sediments of MFM covering the YD period contain abundant aquatic ( $nC_{23}$ ) and  
 278 higher terrestrial ( $nC_{29}$ ) lipid biomarkers ( $n$ -alkanes). Based on the pollen record, the  $nC_{23}$  alkane can  
 279 be related to the aquatic submerged plant *Potamogeton sp.* and the  $nC_{29}$  alkane to leaves originating  
 280 from the terrestrial angiosperm trees *Betula sp.* and *Salix sp.* with input from grasses (Brauer et al.,  
 281 1999a; Diefendorf et al., 2011). For the DUB approach we use the isotopic difference between  $\delta^2H$   
 282 values of the  $nC_{29}$  and of  $nC_{23}$  alkanes ( $\epsilon_{\text{terr-aq}}$ ) as a measure for leaf water  $^2H$  enrichment ( $\Delta^2H_c$ ).

283

284

285

286

287





## 288 4.1 Model parameterization for the MFM application

### 289 4.1.1 Temperature

290

291 Since, no paleotemperature proxy data are directly available for MFM, we use a high-resolution  
292 chironomid based temperature reconstruction from a nearby location, lake Hijkermeer in the  
293 Netherlands, ca. 300 km N of MFM (see the Appendix). The Hijkermeer record is interpreted as a  
294 record of mean July temperatures for Western Europe with an mean error of about 1.59°C (Heiri et al.,  
295 2007). Since leaf wax synthesis occurs most likely during the early part of the growing season (spring  
296 and summer) (Kahmen et al., 2011a; Sachse et al., 2015; Tipple et al., 2013), the Hijkermeer record  
297 might slightly overestimate spring temperatures. However, when reconstructing  $\Delta r_h$  during the  
298 Younger Dryas, it is important that paleotemperature data capture the changes in temperature before  
299 and during that period, rather than absolute temperatures.

300

### 301 4.1.2 Plant physiological parameters

302

303 We estimated plant physiological variables ( $g_s$  and  $r_b$ ) based on literature data from the prevalent  
304 catchment vegetation inferred from available MFM pollen records (Brauer et al., 1999a; Litt and  
305 Stebich, 1999). These suggest that *Betula sp.* and *Salix sp.* were the dominant  $nC_{29}$  producing taxa but  
306 that grasses became more abundant during the YD (Brauer et al., 1999a; Litt and Stebich, 1999).  
307 Reported  $g_s$  values for these species growing under humid to arid conditions today range from 0.1 to  
308 0.5 mol/m<sup>2</sup>/s and boundary layer resistance ( $r_b$ ) values from 0.95 to 1.05 mol/m<sup>2</sup>/s (Klein, 2014;  
309 Schulze, 1982, 1986; Turner, 1984). As input variables for our modified model we therefore used mean  
310 values, i.e. 0.3 mol/m<sup>2</sup>/s for  $g_s$  and 1.0 mol/m<sup>2</sup>/s for  $r_b$ . We used the variance of  $\pm 0.2$  mol/m<sup>2</sup>/s for  $g_s$   
311 and  $\pm 0.1$  mol/m<sup>2</sup>/s for  $r_b$  to calculate the error range of  $\Delta r_h$ . We note the low sensitivity of the DUB  
312 model outcome to variability in these variables (see Fig. 1, Appendix), as such that  $\Delta r_h$  changes of less  
313 than 0.1% result from varying  $g_s$  by 0.4 mol/m<sup>2</sup>/s or  $r_b$  by 0.1 mol/m<sup>2</sup>/s (Fig. 1).

314

### 315 4.2 Estimation of uncertainty

316

317 The estimation of uncertainty for  $\Delta r_h$  is based on a linear error propagation (Eq. (16) - in the  
318 Appendix) using specific error ranges for the individual input variables. For each input variable we  
319 used their individual reported or estimated error (i.e. for chironomid interfered temperature  
320 reconstruction:  $\pm 1.5^\circ\text{C}$ ), for  $\varepsilon_{\text{aq-terr}}$  the analytical uncertainty (standard deviation) of the respective  
321 biomarker  $\delta^2\text{H}$  measurements and for  $g_s$  and  $r_b$  the observed range of plant physiological parameters  
322 between different species ( $g_s$ : 0.1-0.5 mol/m<sup>2</sup>/s,  $r_b$ : 0.95-1.05 m<sup>2</sup>/mol). The resulting average error for  
323  $\Delta r_h$  estimation during the investigated interval is 3.4% (see above and in the Appendix).

324

325

326

327



#### 328 4.3 Model results for the YD period at MFM

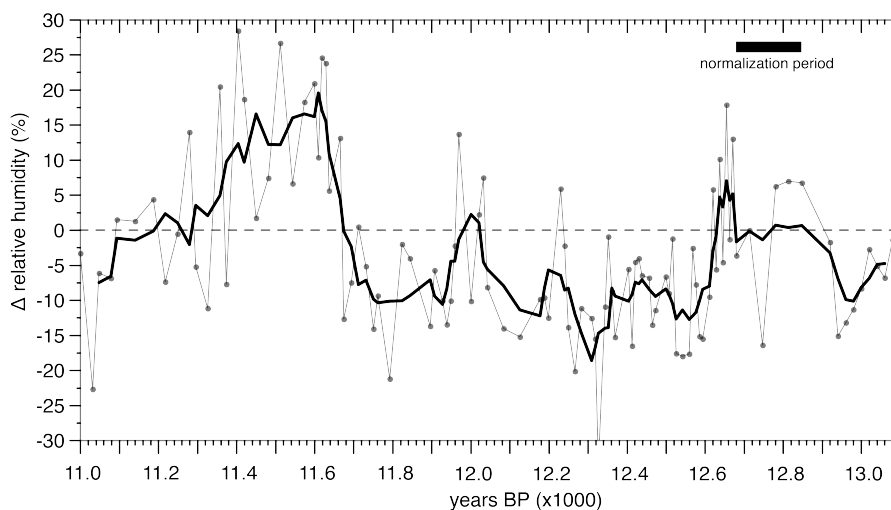
329

330 Applying the DUB approach to the Late Glacial MFM record we can for the first time estimate the  
331 magnitude by which rh changed during a distinct period of abrupt climatic change in the past. Our  
332 quantification revealed substantial changes in relative humidity ( $\Delta rh$ ) on the order of 30% (Fig 2)  
333 during the Late Glacial period, some of which occurred on multi-decadal timescales. To better illustrate  
334 these changes we normalized our results to the mean of the period between 12.847 – 12680 BP (mean  
335 Allerød) (Fig 2), which is thought to have been warmer and moister than the Younger Dryas (Hoek,  
336 2009).

337 In particular, at the onset of the YD at 12.680 years BP,  $\Delta rh$  decreased by 13% +/- 3.4% over 112 years  
338 compared to mean Allerød level (Fig. 2). During the YD (from 12.680-11.600 years BP)  $\Delta rh$  values  
339 were on average 5% +/- 3.4% lower compared to the mean Allerød level. Furthermore in our high-  
340 resolution dataset we observe a division of the YD into two distinct phases: the first part of the YD  
341 (12.610-12.360 years BP) was characterized by low but relatively constant  $\Delta rh$  (variability between -  
342 8% and -13% and a mean of -10%, compared to Allerød), whereas the variability in  $\Delta rh$  increases after  
343 12360 years BP and ranges between -19% and +2% and a mean of -8% compared to Allerød mean  
344 values (Fig. 2). Towards the termination of the YD we reconstructed a strong increase in  $\Delta rh$  (up to  
345 +20% above the Allerød level) over only 80 years. This increase started about 100 years before the YD  
346 – Holocene transition at 11.600 BP (Fig. 2), indicating that hydrological changes lead major ecosystem  
347 changes, which formed the basis for the definition of the YD-Holocene boundary (Brauer et al., 1999a;  
348 Brauer et al., 1999b). The onset of the Holocene was characterized by substantial variability in  $\Delta rh$ ,  
349 with a strong increase followed by a decrease to mean Allerød levels 150 years after the transition. The  
350 reconstructed magnitude of changes, i.e. a ca. 9% reduction in rh during the YD constitutes a shift from  
351 an oceanic to a dry summer climate, comparable to the difference in mean annual rh between Central  
352 and Southern Europe today (Center for Sustainability and the Global Environment (SAGE), 2002; New  
353 et al., 1999). The overall temporal pattern of reconstructed  $\Delta rh$  changes is in good agreement with  
354 proxy data from western Europe (Bakke et al., 2009; Brauer et al., 1999a; Brauer et al., 2008; Goslar  
355 et al., 1993), which indicate a shift to drier conditions due to a southward displacement of the westerly  
356 wind system channelling dry, polar air into Western Europe (Brauer et al., 2008; Rach et al., 2014).

357 Our approach reveals for the first time that substantial changes in rh of up to 20% can take place over  
358 very short time scales, i.e. several decades, leading to substantial changes in terrestrial ecosystems.  
359 While other proxy data reveal qualitative trends in aridification, our approach can be used to identify  
360 hydrological thresholds. Applied to high-resolution records, such as annually laminated lake sediments,  
361 the DUB approach can even be used to derive rates of hydrological changes and compare those with  
362 associated ecological changes (i.e. pollen records).

363



364

365 **Fig 2.** Variability of  $\Delta rh$  during the YD cold period at MFM. The data are normalized to mean Allerød  
366 level (12.847 – 12.680 years BP). The bold line marks the moving average.

367

#### 368 4.4 The effect of vegetation change on $\epsilon_{terr-aq}$ and the estimation of $\Delta rh$

369

370 Numerous studies have established that vegetation changes can also affect the sedimentary leaf wax  
371  $\delta^2H$  record, since significant differences in the net or apparent fractionation ( $\epsilon_{app}$ ) between source water  
372 and lipid  $\delta^2H$  values exist among different plant types, in particular between monocot and dicot (all  
373 grasses) plants (Kahmen et al., 2013b; Tipple et al., 2013). Since the YD period at MFM was  
374 characterized by an increased amount of grasses, we tested, how vegetation changes may affect  $\Delta rh$   
375 reconstructions through the DUB approach. For this we have developed two approaches to “correct”  
376  $\delta^2H_{terr}$  values, based on either a constant offset between monocot and dicot  $\epsilon_{app}$  (Sachse et al., 2012) or  
377 a lower sensitivity of grass derived leaf wax  $\delta^2H$  values to leaf water isotope enrichment (Kahmen et  
378 al., 2013b). Both approaches assume that palynological reconstructions are representative of leaf wax  
379 producing plants and that both monocots and dicots produce similar quantities of *n*-alkanes.

380 We used available palynological data to quantify the relative distribution of major tree vegetation  
381 (*Betula*, *Salix*) and grasses over the investigated period (Fig. 3B), expressed as the fraction of trees and  
382 grasses,  $f_{trees}$  and  $f_{grasses}$ , assuming that leaf waxes and pollen share a similar transport pathway in this  
383 small, constrained crater catchment.

384

##### 385 4.4.1 Correction - case 1 – constant difference in $\epsilon_{app}$ between monocots and dicots

386

387 The first vegetation correction for reconstructed leaf water enrichment ( $\epsilon_{terr-aq}^*$ ) is based on the  
388 assumption of a constant offset in biosynthetic isotope fractionation ( $\epsilon_{bio}$ ) between trees and grasses.  
389 Observational evidence shows that leaf wax lipid  $\delta^2H$  values ( $\delta^2H_{terr}$ ) from C3 monocots are on average  
390 34‰ more negative than from C3 dicots (non-grasses) when growing at the same site (Sachse et al.,



391 2012). This value is based on an observed mean difference between apparent isotope fractionation (i.e.  
 392 The isotopic difference between source water and leaf wax *n* alkanes,  $\epsilon_{app}$ ) values of C3 dicots (-111‰)  
 393 and C3 monocots (-141‰) within a global dataset (Sachse et al., 2012).  
 394 The difference between monocot and dicot *n*-alkane  $\delta^2\text{H}$  could potentially affect our modeled  $\Delta\text{rh}$   
 395 values, especially since an 23% increase in grass abundance in the MFM catchment during the YD has  
 396 been suggested by pollen studies (Brauer et al., 1999a; Litt and Stebich, 1999). The causes for these  
 397 differences in  $\epsilon_{app}$  have been hypothesized to be due to species-specific differences in biosynthetic  
 398 fractionation (Sachse et al., 2012) or temporal differences in leaf wax synthesis during the growing  
 399 season (Tippie et al., 2013). Both scenarios would result in a more or less constant isotopic offset  
 400 between monocots and dicots growing under the same climatic conditions.  
 401 Assuming a mean isotopic difference of -34‰ between trees and grasses (Sachse et al., 2012), we  
 402 calculated a vegetation weighted correction value ( $-34 \cdot f_{grass}$ ) for each data point. This value is then  
 403 subtracted from  $\epsilon_{terr-aq}$ , and results in the vegetation corrected  $\epsilon_{terr-aq}^*$  value (Eq. (14)). Similar  
 404 approaches for a pollen based vegetation reconstruction have been recently proposed and applied  
 405 (Feakins, 2013; Wang et al., 2013).  
 406

$$(14) \quad \epsilon_{terr-aq}^* = \epsilon_{terr-aq} - (-34 \cdot f_{grass})$$

407  
 408 **4.4.2 Correction - case 2: different sensitivity to leaf water isotope enrichment in dicot vs.**  
 409 **monocot leaf wax  $\delta^2\text{H}$  values**  
 410

411 The second vegetation correction ( $\epsilon_{terr-aq}^{**}$ ) is based on the assumption that the isotopic difference  
 412 between monocot and dicot leaf wax *n* alkanes is not constant, but dependant on environmental  
 413 conditions (Kahmen et al., 2013b). Previous greenhouse studies imply that the difference in  $\epsilon_{app}$   
 414 between dicots and monocots is variable depending with a change in humidity conditions (Kahmen et  
 415 al., 2013b). In a high humidity climate chamber treatment (80% rh) monocots and dicots showed  
 416 similar values for  $\epsilon_{app}$  (-220‰ and -214‰ respectively) whereas in a low humidity treatment  $\epsilon_{app}$   
 417 for monocots was substantially lower compared to dicots (-205‰ and -125‰ respectively) (Kahmen et al.,  
 418 2013b), a finding that is in disagreement with the two hypotheses proposed above. Rather, the latter  
 419 study hypothesized that grasses use a mixture of enriched leaf water and unenriched xylem water for  
 420 lipid synthesis (Kahmen et al., 2013b). This hypothesis would imply, that leaf wax *n*-alkane  $\delta^2\text{H}$  values  
 421 of monocots do not record the full magnitude of the evaporative leaf water enrichment signal, but only  
 422 a fraction (Sachse et al., 2009). A recent greenhouse study on grass derived *n*-alkane  $\delta^2\text{H}$  values of a  
 423 broad spectrum of C3 and C4 grasses support this idea (Gamarra et al., 2016). Gamarra et al. suggest  
 424 that the differences between *n*-alkane  $\delta^2\text{H}$  values from grasses and *n*-alkane  $\delta^2\text{H}$  values from  
 425 dicotyledonous plants are caused by an incomplete transfer of leafwater  $\Delta^2\text{H}$  to the *n*-alkanes. As such,  
 426 also a sedimentary record of *n*-alkanes derived partly from grasses would underestimate mean  
 427 ecosystem leaf water enrichment. Under dry conditions this fraction was estimated to be ca. 18% for  
 428 C3 grasses, based on one grass species (Wheat) studied (Kahmen et al., 2013b). The data from  
 429 Gamarra et al. show that for C3 grasses only 38 – 61% of the leaf water evaporative  $^2\text{H}$ -enrichment



430 signal (depending on the species) was transferred to leaf wax *n*-alkane  $\delta^2\text{H}$  values. To work with a  
 431 conservative value and not to overestimate a potential leaf water enrichment signal in grass derived *n*-  
 432 alkane  $\delta^2\text{H}$  values we decided to use the data from Kahmen et al. (2013) for the wheat C3 grass. As  
 433 such our correction approach would rather underestimate changes in relative humidity and represents as  
 434 such the lower limit of reconstructed changes.

435 Under the assumption of different sensitivities to leaf water isotope enrichment of *n*-alkane  $\delta^2\text{H}$  values  
 436 in monocot and dicot plants (Kahmen et al., 2013b) we developed a correction for  $\epsilon_{\text{terr-aq}}$  based on the  
 437 experimentally determined mixing ratio between leaf water and unenriched xylem water in wheat, a C3  
 438 grass (Kahmen et al., 2013b), essentially by weighing the fraction of grass cover with a factor of 0.18:  
 439 (Fig. 3B) (Eq. (15)).

440

$$(15) \quad \epsilon_{\text{terr-aq}}^{**} = (f_{\text{trees}} \cdot 1 + f_{\text{grass}} \cdot 0.18) \cdot \epsilon_{\text{terr-aq}}$$

441

#### 442 4.5 Comparison of results from uncorrected ( $\epsilon_{\text{terr-aq}}$ ) and corrected ( $\epsilon_{\text{terr-aq}}^*$ , $\epsilon_{\text{terr-aq}}^{**}$ ) values

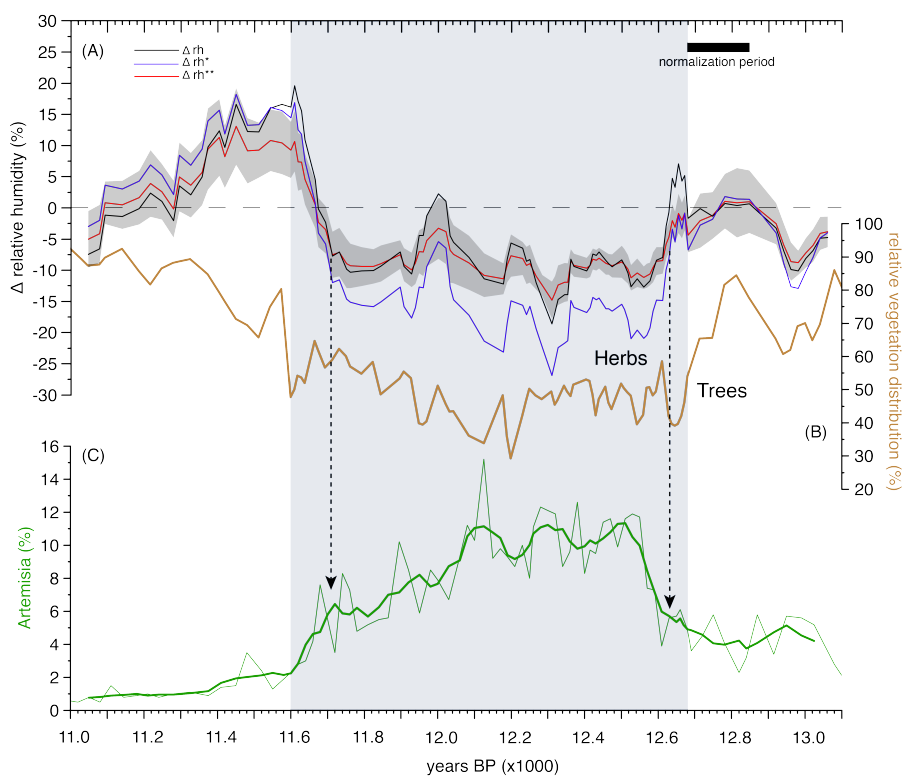
443

444 Results from the raw ( $\Delta\text{rh}$ ) and both vegetation corrected scenarios ( $\Delta\text{rh}^*$  and  $\Delta\text{rh}^{**}$ ) are within the  
 445 calculated error range of 3.4% of  $\Delta\text{rh}$  (Fig. 3A) during the Allerød and the Early Holocene, but diverge  
 446 by up to 10% during the YD, when C3 grass vegetation was estimated to have increased from 28% to  
 447 52% in the catchment of MFM (Fig. 3B). Vegetation corrected results (case 1 Fig. 3A) showed on  
 448 average a 7% stronger decrease for  $\Delta\text{rh}^*$  and only a 2% stronger decrease for  $\Delta\text{rh}^{**}$  compared to  
 449 uncorrected results. As such  $\Delta\text{rh}^{**}$  values (case 2) are within the error range of uncorrected  $\Delta\text{rh}$  during  
 450 the entire record.

451 Interestingly, both correction approaches, but in particular case 2, level the relatively large variability  
 452 in uncorrected  $\Delta\text{rh}$  at the onset and the termination of the YD, where abrupt vegetation changes  
 453 occurred. For example, uncorrected  $\Delta\text{rh}$  changes were predicted to be up to 35% during the termination  
 454 of the YD, corresponding to the modern gradient between western Europe and the semi-desert areas in  
 455 northern Africa (Center for Sustainability and the Global Environment (SAGE), 2002). Vegetation  
 456 corrected  $\Delta\text{rh}^{**}$  values were on the order of 20%, seemingly more reasonably representing local Late  
 457 Glacial changes (Fig. 3A).

458 Our analysis shows that vegetation changes have the potential to affect the DUB approach estimates,  
 459 but a lacking mechanistic understanding of the causes of the differences in  $\delta^2\text{H}_{\text{terr}}$  between tree and  
 460 grass vegetation (Sachse et al., 2012) makes an assessment of the validity of either (or any) correction  
 461 approach difficult. Tentatively, the lower variability in  $\Delta\text{rh}^{**}$  within the YD as well as the less  
 462 pronounced shift in particular at the onset and termination of the YD (Fig. 3A) provides are more  
 463 realistic scenario. But as of now, we regard the differences in predictions as the error of quantitative  
 464 predictions from the DUB approach. This uncertainty is larger during periods characterized by  
 465 vegetation changes and in our case maximum differences in prediction of  $\Delta\text{rh}$  between the Allerød and  
 466 the YD are on the order of 11% (mean Allerød vs mean YD difference between  $\Delta\text{rh}$  and  $\Delta\text{rh}^*$ ).

467



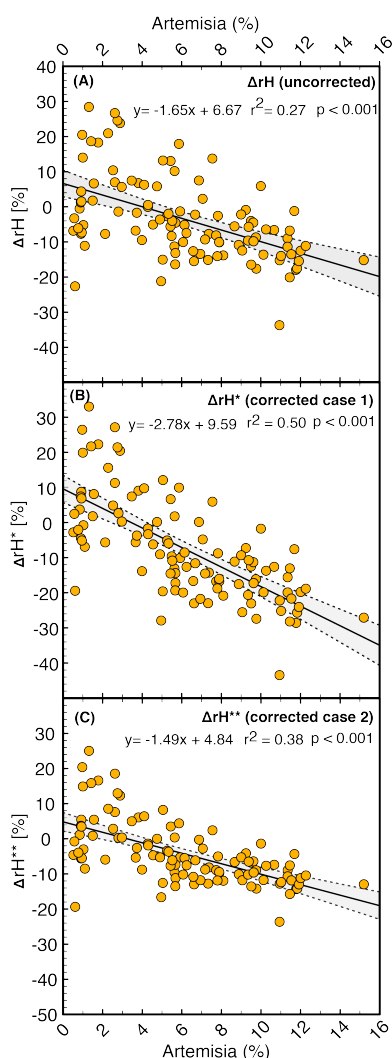
468  
 469 **Fig. 3:** (A) Reconstructed  $\Delta rh$  variability during the YD period, without vegetation correction (**black**  
 470 **line,  $\Delta rh$** ) with vegetation correction assuming a constant offset between C3 dicots and C3 monocots  
 471 (**blue line,  $\Delta rh^*$** ), with vegetation correction assuming different leaf water sensitivities among grasses  
 472 and trees (**red line,  $\Delta rh^{**}$** ). The shaded area marks the error range for  $\Delta rh^{**}$ . (B) relative distribution  
 473 of trees and grasses in the catchment of MFM during the YD from pollen studies (Brauer et al., 1999a;  
 474 Litt and Stebich, 1999). (C) Occurrence of *Artemisia* pollen in the catchment of MFM during YD  
 475 (Brauer et al., 1999a; Litt and Stebich, 1999). Arrows highlight the contemporaneous major changes in  
 476  $\Delta rh$  and *Artemisia*.

477  
 478 **4.6 Comparison of reconstructed  $\Delta rh$  with other proxy data**  
 479

480 We can further demonstrate the validity of our approach by direct comparison to other hydroclimate  
 481 proxies from the MFM record. For example, a classical palynological marker for more arid conditions  
 482 is *Artemisia* pollen (D'Andrea et al., 2003). In the MFM catchment a prominent increase in the  
 483 occurrence of *Artemisia* has been used to infer dryer conditions during the YD (Fig. 3C) (Brauer et al.,  
 484 1999a; Litt and Stebich, 1999), (Bremer and Humphries, 1993; D'Andrea et al., 2003). When  
 485 comparing the abundance of *Artemisia* pollen % (note that the *Artemisia* abundance data are not part of  
 486 the vegetation corrections discussed above) to the DUB  $\Delta rh$  record, we observed striking similarities  
 487 over the whole of the study period (Fig. 3A,C). Inferred wetter conditions during the second phase of



488 the YD, or centennial scale excursions to higher  $\Delta rh$  (such as between 12280 and 12170 years BP) go  
489 in line with lower *Artemisia* pollen abundance after 12.100 BP. In fact, both independent datasets show  
490 an inverse, statistically significant relationship ( $p < 0.001$ ) (Fig. 4A-C), with high *Artemisia* pollen  
491 abundance during periods of low  $\Delta rh$  values (Fig. 3A,C). The correlation between  $\Delta rh$  and *Artemisia* is  
492 higher for vegetation corrected  $\Delta rh^*$  and  $\Delta rh^{**}$  (Fig. 4B,C) than uncorrected  $\Delta rh$  and in particular for  
493  $\Delta rh^{**}$  the variance of the dataset is greatly reduced (Fig. 4C), providing support for the hypothesis that  
494 vegetation changes could have affected the record.  
495



496  
497 **Fig. 4:** Correlation plots of normalized reconstructed  $\Delta rh$  vs. *Artemisia* population. (A) uncorrected  $\Delta rh$   
498 values vs. *Artemisia*. (B) vegetation corrected  $\Delta rh$  values ( $\Delta rh^*$ ) vs *Artemisia*. (C) Vegetation corrected  
499  $\Delta rh$  values ( $\Delta rh^{**}$ ) vs *Artemisia*.  
500



501 **5. Conclusions**

502

503 We present a novel approach for quantifying paleohydrological changes (i.e. changes in relative  
504 humidity) combining sedimentary lipid biomarker  $\delta^2\text{H}$  values from aquatic and terrestrial lipids with  
505 mechanistic leaf water isotope modeling. This dual-biomarker approach (DUB) relies on the  
506 observation that aquatic and terrestrial organisms within the catchment of small lakes from temperate  
507 climate zones use distinct water sources, namely lake (i.e. precipitation) and  $^2\text{H}$ -enriched leaf water as  
508 a source for their organic hydrogen. By taking advantage of the mechanistic understanding of and  
509 available models on leaf water isotope enrichment in terrestrial plants, we show it is possible to extract  
510 quantitative information about changes in relative humidity from sedimentary records.

511 Parameterizing and applying the DUB model to a lacustrine lipid biomarker  $\delta^2\text{H}$  record from western  
512 Europe, we find strong and abrupt changes in rh at the onset and the termination of the YD occurring  
513 within the lifetime of a human generation. Specifically, our approach showed that shifts in rh of up to  
514 13% +/- 3.4% occurred within only 112 years. This dramatic change corresponds to shifts in average  
515 biome rh from oceanic to dry summer climates. Our quantification showed that dry conditions  
516 prevailed during the Younger Dryas period with rh being between 8 and 15% lower on average  
517 compared to the Allerød, depending on how the possible effect of vegetation changes is accounted for.  
518 The pattern but also the magnitude of our rh reconstruction agrees well with other proxy data, such as  
519 the increase in the abundance of specific taxa adapted to dry conditions (e.g. *Artemisia*) during that  
520 time period.

521 Our analyses shows that the DUB approach is capable of quantifying past hydrological changes in  
522 temperate environments, when additional proxy data, especially on vegetation distribution and  
523 paleotemperature exist. We suggest that this approach can be particularly valuable in the future for the  
524 validation of climate models and to better understand uncertainties in predictions of future hydrological  
525 change under global warming.

526

527

528 **Appendix**

529

530 **Error propagation**

531

532 The uncertainty estimation ( $\Delta f$ , Eq. (16)) for the reconstructed  $\Delta rh$  variability is based on a linear error  
533 propagation, which is the most conservative method for error estimations. This Method does not  
534 require the same kind of the considered errors and provides therefore the possibility to combine  
535 different kinds of errors with their specific ranges (i.e. measuring error, counting error, etc.). The  
536 individual error ranges of the independent variables in our approach arise from different sources such  
537 as analytical errors (chironomid interfered temperature reconstruction:  $\pm 1.5^\circ\text{C}$ ), observed variations of  
538 plant physiological parameters between different species (stomatal conductance: 0.1-0.5 mol/m<sup>2</sup>/s,  
539 boundary layer resistance: 0.95-1.05 m<sup>2</sup>/mol) and standard deviation of  $\delta^2\text{H}$  measurements of  
540 terrestrial and aquatic *n*-alkanes.





541 The specific uncertainty for  $\varepsilon_{terr-aq}^{**}$  was preliminary determined by a separate error propagation using  
 542 the (analytical) standard deviation of the triplicate measurements of the sedimentary  $n$ -alkane  $\delta^2H$   
 543 values as well as the plant derived  $n$ -alkane  $\delta^2H$  measurements by Kahmen et al 2013. The results of  
 544 these separate error estimation were integrated into the general error estimation of  $\Delta rh^{**}$ .

545 In contrast to the linear error propagation a less conservative method (Gaussian error propagation)  
 546 requires a similarity of the errors, i.e. all errors are measurement or counting errors, which is not the  
 547 case in this study. The mean error when using the Gaussian method is however only 3.2% and therefore  
 548 only 0.2% smaller than the calculated error using the linear propagation.

549

$$(16) \Delta f = \left| \frac{\partial rh}{\partial \varepsilon_{terr-aq}} \right| \cdot \Delta \varepsilon_{terr-aq}^{**} + \left| \frac{\partial rh}{\partial r_b} \right| \cdot \Delta r_b + \left| \frac{\partial rh}{\partial g_s} \right| \cdot \Delta g_s + \left| \frac{\partial rh}{\partial T_{air}} \right| \cdot \Delta T_{air}$$

550

#### 551 **Temperature data**

552

553 The temperature data used for the DUB model parameterization of the MFM case were taken from ref.  
 554 35 and constitute reconstructed summer temperatures based on chironomid analyses from Hijkermeer  
 555 (NL) (Heiri et al. (2007)), which, to our knowledge, constitutes the closest lateglacial paleotemperature  
 556 record to the MFM site (distance 311km). However, the dataset of the Hijkermeer consists only of 37  
 557 data-points between 13.000 BP and 11.000 BP with a temporal resolution varying between 26 to 167  
 558 years /sample. Therefore, we determined a new equidistant time-series for the temperature data, fitting  
 559 data-volume and temporal resolution of our  $\Delta^2H_e$  record from MFM (106 data-points with an 8 to 33  
 560 year-resolution). For calculating the equidistant time series we were using method “interpl” with the  
 561 specification “linear” in MATLAB (version R2010b).

562

563

#### 564 **Vegetation data**

565 Information about Lateglacial vegetation-cover in the catchment area of MFM is based on  
 566 palynological analyses (Brauer et al. (1999), Litt & Stebich (1999)). We used Pollen percent data also  
 567 for determining the vegetation distribution between trees and grasses for each datapoint. For using  
 568 these vegetation data in our model it was necessary to determine an equidistant time-series according to  
 569 age model of our  $\Delta^2H_e$  values. For calculating these time series we used also method “interpl” with the  
 570 specification “linear” in MATLAB (version R2010b).

571

#### 572 **Author contributions**

573 Oliver Rach conducted model modifications, calculations and wrote the paper. Ansgar Kahmen  
 574 provided the basic leaf water enrichment model and was responsible for plant physiological part and  
 575 contributed in writing the paper. Achim Brauer was responsible for lake coring, provided the  
 576 chronology and stratigraphy for Younger Dryas hydrological reconstruction and wrote the paper. Dirk  
 577 Sachse conceived the research, acquired financial support and wrote the paper.



578 **Competing financial interests**

579 The authors declare no competing financial interests.

580

581 **Acknowledgements**

582

583 This work was supported by a DFG Emmy-Noether grant (SA1889/1-1) and an ERC Consolidator  
584 Grant (No. 647035 *STEEP*clim) to D.S. It is a contribution to the INTIMATE project, which was  
585 financially supported as EU COST Action ES0907 and to the Helmholtz Association (HGF) Climate  
586 Initiative REKLIM Topic 8, Rapid climate change derived from proxy data, and has used infrastructure  
587 of the HGF TERENO program.

588

589 **References**

590 Aichner, B., Herzschuh, U., Wilkes, H., Vieth, A. and Böhner, J. (2010)  $\delta D$  values of n-alkanes in  
591 Tibetan lake sediments and aquatic macrophytes - A surface sediment study and application to a 16 ka  
592 record from Lake Koucha. *Organic Geochemistry* 41, 779-790.

593 Alley, R.B. (2000) Ice-core evidence of abrupt climate changes. *Proc. Natl. Acad. Sci. U. S. A.* 97,  
594 1331-1334.

595 Alley, R.B. and Cuffey, K.M. (2001) Oxygen- and Hydrogen-Isotopic Ratios of Water in Precipitation:  
596 Beyond Paleothermometry. *Reviews in Mineralogy and Geochemistry* 43, 527-553.

597 Bakke, J., Lie, O., Heegaard, E., Dokken, T., Haug, G.H., Birks, H.H., Dulski, P. and Nilsen, T. (2009)  
598 Rapid oceanic and atmospheric changes during the Younger Dryas cold period. *Nature Geoscience* 2,  
599 202-205.

600 Barbour, M.M. (2007) Stable oxygen isotope composition of plant tissue: a review. *Funct. Plant Biol.*  
601 34, 83-94.

602 Blaga, C.I., Reichert, G.J., Lotter, A.F., Anselmetti, F.S. and Damste, J.S.S. (2013) A TEX86 lake  
603 record suggests simultaneous shifts in temperature in Central Europe and Greenland during the last  
604 deglaciation. *Geophysical Research Letters* 40, 948-953.

605 Bowen, G.J. (2008) Spatial analysis of the intra-annual variation of precipitation isotope ratios and its  
606 climatological corollaries. *J. Geophys. Res.-Atmos.* 113.

607 Brauer, A., Endres, C., Günter, C., Litt, T., Stebich, M. and Negendank, J.F.W. (1999a) High resolution  
608 sediment and vegetation responses to Younger Dryas climate change in varved lake sediments from  
609 Meerfelder Maar, Germany. *Quaternary Science Reviews* 18, 321-329.

610 Brauer, A., Endres, C. and Negendank, J.F.W. (1999b) Lateglacial calendar year chronology based on  
611 annually laminated sediments from Lake Meerfelder Maar, Germany. *Quaternary International* 61, 17-  
612 25.

613 Brauer, A., Haug, G.H., Dulski, P., Sigman, D.M. and Negendank, J.F.W. (2008) An abrupt wind shift  
614 in western Europe at the onset of the Younger Dryas cold period. *Nature Geoscience* 1, 520-523.

615 Bremer, K. and Humphries, C.J. (1993) *Generic Monograph of the Asteraceae-Anthemideae*. The  
616 Natural History Museum.

617 Bush, R.T. and McInerney, F.A. (2013) Leaf wax n-alkane distributions in and across modern plants:  
618 Implications for paleoecology and chemotaxonomy. *Geochimica et Cosmochimica Acta* 117, 161-179.



- 619 Center for Sustainability and the Global Environment (SAGE) (2002) Atlas of the biosphere - Average  
620 Annual Relative Humidity - <http://www.sage.wisc.edu>. Nelson Institute for Environmental  
621 Studies - University of Wisconsin, The Board of Regents of the University of Wisconsin System.
- 622 Craig, G.L. (1965) Deuterium and oxygen 18 variations in the ocean and the marine atmosphere, in:  
623 Tongiari, E. (Ed.), Stable Isotopes in Oceanographic Studies and Paleotemperatures. CNR Lab. Geol.  
624 Nucl., Pisa, pp. 9–130.
- 625 D'Andrea, S., Caramiello, R., Ghignone, S. and Siniscalco, C. (2003) Systematic studies on some  
626 species of the genus *Artemisia*: biomolecular analysis. *Plant Biosystems - An International Journal*  
627 *Dealing with all Aspects of Plant Biology* 137, 121-130.
- 628 Dawson, T.E. (1993) Hydraulic lift and water-use by plants - Implications for water-balance,  
629 performance and plant-plant interactions. *Oecologia* 95, 565-574.
- 630 Diefendorf, A.F., Freeman, K.H., Wing, S.L. and Graham, H.V. (2011) Production of n-alkyl lipids in  
631 living plants and implications for the geologic past. *Geochimica et Cosmochimica Acta* 75, 7472-7485.
- 632 Eglinton, G. and Hamilton, R.J. (1967) Leaf epicuticular waxes. *Science* 156, 1322-1327.
- 633 Farquhar, G.D., Cernusak, L.A. and Barnes, B. (2007) Heavy water fractionation during transpiration.  
634 *Plant Physiol.* 143, 11-18.
- 635 Feakins, S.J. (2013) Pollen-corrected leaf wax D/H reconstructions of northeast African hydrological  
636 changes during the late Miocene. *Paleogeogr. Paleoclimatol. Paleoecol.* 374, 62-71.
- 637 Ferrio, J.P., Cuntz, M., Offermann, C., Siegwolf, R., Saurer, M. and Gessler, A. (2009) Effect of water  
638 availability on leaf water isotopic enrichment in beech seedlings shows limitations of current  
639 fractionation models. *Plant Cell and Environment* 32, 1285-1296.
- 640 Ficken, K.J., Li, B., Swain, D.L. and Eglinton, G. (2000) An n-alkane proxy for the sedimentary input  
641 of submerged/floating freshwater aquatic macrophytes. *Organic Geochemistry* 31, 745-749.
- 642 Gamarra, B., Sachse, D. and Kahmen, A. (2016) Effects of leaf water evaporative 2H-enrichment and  
643 biosynthetic fractionation on leaf wax n-alkane  $\delta^2\text{H}$  values in C3 and C4 grasses. *Plant, Cell &*  
644 *Environment*.
- 645 Gao, L., Hou, J., Toney, J., MacDonald, D. and Huang, Y. (2011) Mathematical modeling of the  
646 aquatic macrophyte inputs of mid-chain n-alkyl lipids to lake sediments: Implications for interpreting  
647 compound specific hydrogen isotopic records. *Geochimica et Cosmochimica Acta* 75, 3781-3791.
- 648 Gat, J.R. (1996) Oxygen and Hydrogen isotopes in the hydrologic cycle. *Annual Review of Earth and*  
649 *Planetary Sciences* 24, 225-262.
- 650 Goslar, T., Kuc, T., Ralska-Jasiewiczowa, M., Ryznar, K., Arnold, M., Bard, E., van Geel, B.,  
651 Pazdur, M., Szeroczyńska, K., Wicik, B., Wikłowski, K. and Walanus, A. (1993) High-  
652 resolution lacustrine record of the late glacial/holocene transition in central Europe. *Quaternary Science*  
653 *Reviews* 12, 287-294.
- 654 Heiri, O., Brooks, S.J., Renssen, H., Bedford, A., Hazekamp, M., Ilyashuk, B., Jeffers, E.S., Lang, B.,  
655 Kirilova, E., Kuiper, S., Millet, L., Samartin, S., Toth, M., Verbruggen, F., Watson, J.E., van Asch, N.,  
656 Lammertsma, E., Amon, L., Birks, H.H., Birks, H.J.B., Mortensen, M.F., Hoek, W.Z., Magyari, E.,  
657 Muñoz Sobrino, C., Seppä, H., Tinner, W., Tonkov, S., Veski, S. and Lotter, A.F. (2014) Validation of  
658 climate model-inferred regional temperature change for late-glacial Europe. *Nat Commun* 5.
- 659 Heiri, O., Cremer, H., Engels, S., Hoek, W.Z., Peeters, W. and Lotter, A.F. (2007) Lateglacial summer  
660 temperatures in the Northwest European lowlands: a chironomid record from Hijkermeer, the  
661 Netherlands. *Quaternary Science Reviews* 26, 2420-2437.



- 662 Hoek, W. (2009) Bølling-Allerød Interstadial, in: Gornitz, V. (Ed.), Encyclopedia of Paleoclimatology  
 663 and Ancient Environments. Springer Netherlands, pp. 100-103.
- 664 IAEA/WMO (2006) Global Network of Isotopes in Precipitation. The GNIP Database, Bundesanstalt  
 665 fuer Gewaesserkunde.
- 666 IPCC (2015) Intergovernmental panel on climate change, <http://www.IPCC.ch>.
- 667 Jackson, R.B., Canadell, J., Ehleringer, J.R., Mooney, H.A., Sala, O.E. and Schulze, E.D. (1996) A  
 668 global analysis of root distributions for terrestrial biomes. *Oecologia* 108, 389-411.
- 669 Jacob, H. and Sonntag, C. (1991) An 8-year record of the seasonal-variation of H-2 and O-18 in  
 670 atmospheric water-vapor and precipitation at Heidelberg, Germany. *Tellus Series B-Chemical and*  
 671 *Physical Meteorology* 43, 291-300.
- 672 Jacob, J., Huang, Y., Disnar, J.-R., Sifeddine, A., Boussafir, M., Spadano Albuquerque, A.L. and  
 673 Turcq, B. (2007) Paleohydrological changes during the last deglaciation in Northern Brazil. *Quaternary*  
 674 *Science Reviews* 26, 1004-1015.
- 675 Jasechko, S., Sharp, Z.D., Gibson, J.J., Birks, S.J., Yi, Y. and Fawcett, P.J. (2013) Terrestrial water  
 676 fluxes dominated by transpiration. *Nature* 496, 347-+.
- 677 Jones, H.G. (2013) *Plants and Microclimate: A Quantitative Approach to Environmental Plant*  
 678 *Physiology*. Cambridge University Press.
- 679 Kahmen, A., Dawson, T.E., Vieth, A. and Sachse, D. (2011a) Leaf wax n-alkane delta D values are  
 680 determined early in the ontogeny of *Populus trichocarpa* leaves when grown under controlled  
 681 environmental conditions. *Plant Cell and Environment* 34, 1639-1651.
- 682 Kahmen, A., Hoffmann, B., Schefuss, E., Arndt, S.K., Cernusak, L.A., West, J.B. and Sachse, D.  
 683 (2013a) Leaf water deuterium enrichment shapes leaf wax n-alkane delta D values of angiosperm  
 684 plants II: Observational evidence and global implications. *Geochimica et Cosmochimica Acta* 111, 50-  
 685 63.
- 686 Kahmen, A., Sachse, D., Arndt, S.K., Tu, K.P., Farrington, H., Vitousek, P.M. and Dawson, T.E.  
 687 (2011b) Cellulose delta(18)O is an index of leaf-to-air vapor pressure difference (VPD) in tropical  
 688 plants. *Proceedings of the National Academy of Sciences* 108, 1981-1986.
- 689 Kahmen, A., Schefuss, E. and Sachse, D. (2013b) Leaf water deuterium enrichment shapes leaf wax n-  
 690 alkane delta D values of angiosperm plants I: Experimental evidence and mechanistic insights.  
 691 *Geochimica et Cosmochimica Acta* 111, 39-49.
- 692 Kahmen, A., Simonin, K., Tu, K., Goldsmith, G.R. and Dawson, T.E. (2009) The influence of species  
 693 and growing conditions on the 18-O enrichment of leaf water and its impact on 'effective path length'.  
 694 *New Phytologist* 184, 619-630.
- 695 Kanner, L.C., Burns, S.J., Cheng, H., Edwards, R.L. and Vuille, M. (2013) High-resolution variability  
 696 of the South American summer monsoon over the last seven millennia: insights from a speleothem  
 697 record from the central Peruvian Andes. *Quaternary Science Reviews* 75, 1-10.
- 698 Klein, T. (2014) The variability of stomatal sensitivity to leaf water potential across tree species  
 699 indicates a continuum between isohydric and anisohydric behaviours. *Functional Ecology* 28, 1313-  
 700 1320.
- 701 Leuzinger, S. and Korner, C. (2007) Tree species diversity affects canopy leaf temperatures in a mature  
 702 temperate forest. *Agricultural and Forest Meteorology* 146, 29-37.
- 703 Litt, T. and Stebich, M. (1999) Bio- and chronostratigraphy of the lateglacial in the Eifel region,  
 704 Germany. *Quaternary International* 61, 5-16.



- 705 New, M., Hulme, M. and Jones, P. (1999) Representing Twentieth-Century Space–Time Climate  
 706 Variability. Part I: Development of a 1961–90 Mean Monthly Terrestrial Climatology. *Journal of*  
 707 *Climate* 12, 829-856.
- 708 Peters, K.E., Moldowan, J.M. and Walters, C.C. (2007) *The Biomarker Guide: Volume 1, Biomarkers*  
 709 *and Isotopes in the Environment and Human History*. Cambridge University Press.
- 710 Rach, O., Brauer, A., Wilkes, H. and Sachse, D. (2014) Delayed hydrological response to Greenland  
 711 cooling at the onset of the Younger Dryas in western Europe. *Nature Geoscience* 7, 109-112.
- 712 Sachse, D., Billault, I., Bowen, G.J., Chikaraishi, Y., Dawson, T.E., Feakins, S.J., Freeman, K.H.,  
 713 Magill, C.R., McInerney, F.A., van der Meer, M.T.J., Polissar, P., Robins, R.J., Sachs, J.P., Schmidt,  
 714 H.-L., Sessions, A.L., White, J.W.C., West, J.B. and Kahmen, A. (2012) Molecular Paleohydrology:  
 715 Interpreting the Hydrogen-Isotopic Composition of Lipid Biomarkers from Photosynthesizing  
 716 Organisms. *Annual Review of Earth and Planetary Sciences* 40, 221-249.
- 717 Sachse, D., Dawson, M.N. and Kahmen, A. (2015) Seasonal variation of leaf wax n-alkane production  
 718 and  $\delta^2\text{H}$  values from the evergreen oak tree, *Quercus agrifolia*. *Isotopes in Environmental & Health*  
 719 *Studies* in press.
- 720 Sachse, D., Kahmen, A. and Gleixner, G. (2009) Significant seasonal variation in the hydrogen isotopic  
 721 composition of leaf-wax lipids for two deciduous tree ecosystems (*Fagus sylvatica* and *Acer*  
 722 *pseudoplatanus*). *Organic Geochemistry* 40, 732-742.
- 723 Sachse, D., Radke, J. and Gleixner, G. (2004) Hydrogen isotope ratios of recent lacustrine sedimentary  
 724 n-alkanes record modern climate variability. *Geochimica et Cosmochimica Acta* 68, 4877-4889.
- 725 Sachse, D., Radke, J. and Gleixner, G. (2006)  $\delta\text{D}$  values of individual n-alkanes from terrestrial plants  
 726 along a climatic gradient - Implications for the sedimentary biomarker record. *Organic Geochemistry*  
 727 37, 469-483.
- 728 Schefuss, E., Kuhlmann, H., Mollenhauer, G., Prange, M. and Pätzold, J. (2011) Forcing of wet phases  
 729 in southeast Africa over the past 17,000 years. *Nature* 480, 509-512.
- 730 Scherrer, D., Bader, M.K.F. and Korner, C. (2011) Drought-sensitivity ranking of deciduous tree  
 731 species based on thermal imaging of forest canopies. *Agricultural and Forest Meteorology* 151, 1632-  
 732 1640.
- 733 Schulze, E.D. (1986) Carbon dioxide and water vapor exchange in response to drought in the  
 734 atmosphere and in the soil. *Annual Review of Plant Physiology and Plant Molecular Biology* 37, 247-  
 735 274.
- 736 Schulze, E.D., Hall, A. E. (1982) Stomatal response, water loss and  $\text{CO}_2$  assimilation rates of plants in  
 737 contrasting environments. *Encyclopedia of Plant Physiology* 12B, 181-230.
- 738 Seki, O., Meyers, P.A., Yamamoto, S., Kawamura, K., Nakatsuka, T., Zhou, W. and Zheng, Y. (2011)  
 739 Plant-wax hydrogen isotopic evidence for postglacial variations in delivery of precipitation in the  
 740 monsoon domain of China. *Geology* 39, 875-878.
- 741 Song, X., Barbour, M.M., Farquhar, G.D., Vann, D.R. and Helliker, B.R. (2013) Transpiration rate  
 742 relates to within- and across-species variations in effective path length in a leaf water model of oxygen  
 743 isotope enrichment. *Plant Cell and Environment* 36, 1338-1351.
- 744 Tipple, B.J., Berke, M.A., Doman, C.E., Khachatryan, S. and Ehleringer, J.R. (2013) Leaf-wax n-  
 745 alkanes record the plant–water environment at leaf flush. *Proceedings of the National Academy of*  
 746 *Sciences* 110, 2659-2664.
- 747 Turner, N.C., Schulze, E. D., & Gollan, T. (1984) The responses of stomata and leaf gas exchange to  
 748 vapour pressure deficits and soil water content. *Oecologia* 63(3), 338-342.



- 749 Tyler, J.J., Leng, M.J., Sloane, H.J., Sachse, D. and Gleixner, G. (2008) Oxygen isotope ratios of  
750 sedimentary biogenic silica reflect the European transcontinental climate gradient. *Journal of*  
751 *Quaternary Science* 23, 341-350.
- 752 von Grafenstein, U., Erlenkeuser, H., Brauer, A., Jouzel, J. and Johnsen, S.J. (1999) A mid-European  
753 decadal isotope-climate record from 15,500 to 5000 years BP. *Science* 284, 1654-1657.
- 754 Wang, Y.V., Larsen, T., Leduc, G., Andersen, N., Blanz, T. and Schneider, R.R. (2013) What does leaf  
755 wax  $\delta D$  from a mixed C3/C4 vegetation region tell us? *Geochimica et Cosmochimica Acta* 111, 128-  
756 139.
- 757 Zhang, X.N., Gillespie, A.L. and Sessions, A.L. (2009) Large D/H variations in bacterial lipids reflect  
758 central metabolic pathways. *Proc. Natl. Acad. Sci. U. S. A.* 106, 12580-12586.
- 759 Zhang, Z. and Sachs, J.P. (2007) Hydrogen isotope fractionation in freshwater algae: I. Variations  
760 among lipids and species. *Organic Geochemistry* 38, 582-608.  
761  
762